Experimentation with tension-only devices for use with seismic energy dissipation systems

J. Cook, G.W. Rodgers, G.A. MacRae & J.G. Chase

Departments of Mechanical and Civil Engineering, University of Canterbury, Christchurch, New Zealand.

ABSTRACT: Seismic damage-resistant structures, such as jointed precast connections and rocking wall structures, usually require supplementary energy dissipation devices to limit peak displacements. Yielding steel fuses or buckling restrained braces (BRBs) can provide energy dissipation but have a tendency to create residual compressive forces after joint closing that can resist the re-centring of the structure and fight the post-tensioning forces on subsequent cycles. A ratcheting, tension-only device has been developed to offer resistance to loading in tension, while offering negligible resistance to compressive motion, and can be used in conjunction with a range of energy dissipation mechanisms. This lack of compressive forces allows re-seating of a rocking connection to minimise residual structural displacements. Upon re-loading, fuse engagement will be more rapid due to the ratcheting mechanism, as the absence of residual compressive loads reduces the amount of elastic take-up before yielding occurs. A tension-only solution also removes the requirement for buckling restraint to be designed into the fuse element. Two prototype ratcheting mechanisms have been designed and experimentally tested in an MTS-810 test machine with fuses providing a yield force of 45 kN and an ultimate tensile force of 65 kN. Experimental proof-of-concept testing on fourteen fuse elements demonstrated the function of the ratcheting mechanisms and assessed the hysteretic behaviour of each system. The influence of tooth pitch is investigated experimentally, varying from 3-40 mm in the different prototypes.

1 INTRODUCTION

The capital cost of the Canterbury earthquakes of 2010 and 2011 has been estimated to be as high as $40 billion (NZ Treasury 2014). The extent of the damage and operational disruption has led to an increased public expectation regarding the resilience of structures to earthquakes. Low damage structural technology is a large field covering much of the work towards improving building performance levels following seismic events (CERC 2012).

A key concept in such technology is the idea of providing specific energy dissipation mechanisms to absorb earthquake energy and reduce the damage to a structure. Supplementary energy dissipation is commonly provided for structures through the use of four broadly categorised types of dampers (Symans, et al. 2008). These dampers are viscous fluid dampers (Lee and Taylor 2001), viscoelastic solid dampers (Kanitkar, et al. 2006), yielding steel (Black, et al 2004), and friction dampers, such as sliding hinge joints (Clifton 2005). A further category that is gaining interest is the use of extrusion dampers, such as the high force-to-volume (HF2V) lead-extrusion damper (Rodgers, et al. 2008).

Metallic dampers or yielding steel fuses remain a desirable option due to the familiarity of the behaviour of steel under loading, and their general simplicity in design. However, a key issue with some common approaches, such as with buckling restrained braces (BRBs), is the presence of residual compressive stresses after a seismic event. Such stresses limit the effectiveness of the device to allow the centring of a structure post-quake, and also impair their performance in subsequent loading cycles.

Slender bracing that yields in tension and buckles elastically in compression removes these residual compressive forces. However, plastic deformation on prior cycles increases the unstressed member length and results in a dead-zone with take-up on subsequent cycles. Therefore, subsequent cycles will provide delayed engagement and reduced energy dissipation capacity.

One way to address these issues is the use of a tension only, steel dissipation device, where dissipation

occurs due to mechanisms such as yielding or friction. This concept, originally referred to as a Grip 'n' Grab (GnG) device, was modelled for a rocking system (Gunning and Weston 2013). However, it was only a computational investigation and no prototype was investigated.

Other tension-only damper/bracing research considered hysteretic dampers (Phocas and Pocanschi 2003) and seesaw systems (Kang and Tagawa 2012). Recent research produced newer developments, including adding self-centring capability to BRB systems (Eatherton, et al. 2014), using wedge spring devices to offset anchor bolt elongation in column connections (Lei, et al. 2014) and a non-buckling segmented brace system with sliding joints (Hao, 2015). However, the proposed device and prototype presented in this work offers a novel alternative that aims to be a simple, cost-effective solution for industry.

2 DEVICE DESIGN

Two prototype designs show a progression of functionality and use of space. The first GnG ratcheting, yielding fuse device makes use of a linear ratcheting mechanism to achieve the desired single direction engagement. This mechanism allows the device to engage in tension, offering resistance to motion acting to displace a structure, while providing negligible impediment to any restoring motion.

A number of concepts were considered for the ratchet mechanism including designs making use of friction-based or stepped interfaces. Particular attention was given to reliable engagement, low manufacturing cost and robustness of the design concepts. The initial chosen design is comprised of two pawls and a rack with teeth on both sides. A tension spring fitted between the pawls is used to aid initial engagement during tensile loading. Upon initial engagement the ratchet mechanism locks tighter as the engagement interface is self-stabilising and the tension spring provides initial engagement only. The two pawls rotate about pins located by a main support made from a standard RHS section. A circular yielding steel fuse element is attached to the rack, and each end of the device has a rectangular tongue for mounting in the MTS-810 test machine. Tensile forces in the fuse are transferred to the rack, which induces compressive forces in the pawls. These forces then transfer into the main support body via bearing contact areas on the pawl pins. Cap screws connect the cover plate with the main support body and the upper tongue. Figure 1a shows the assembly of the first prototype.
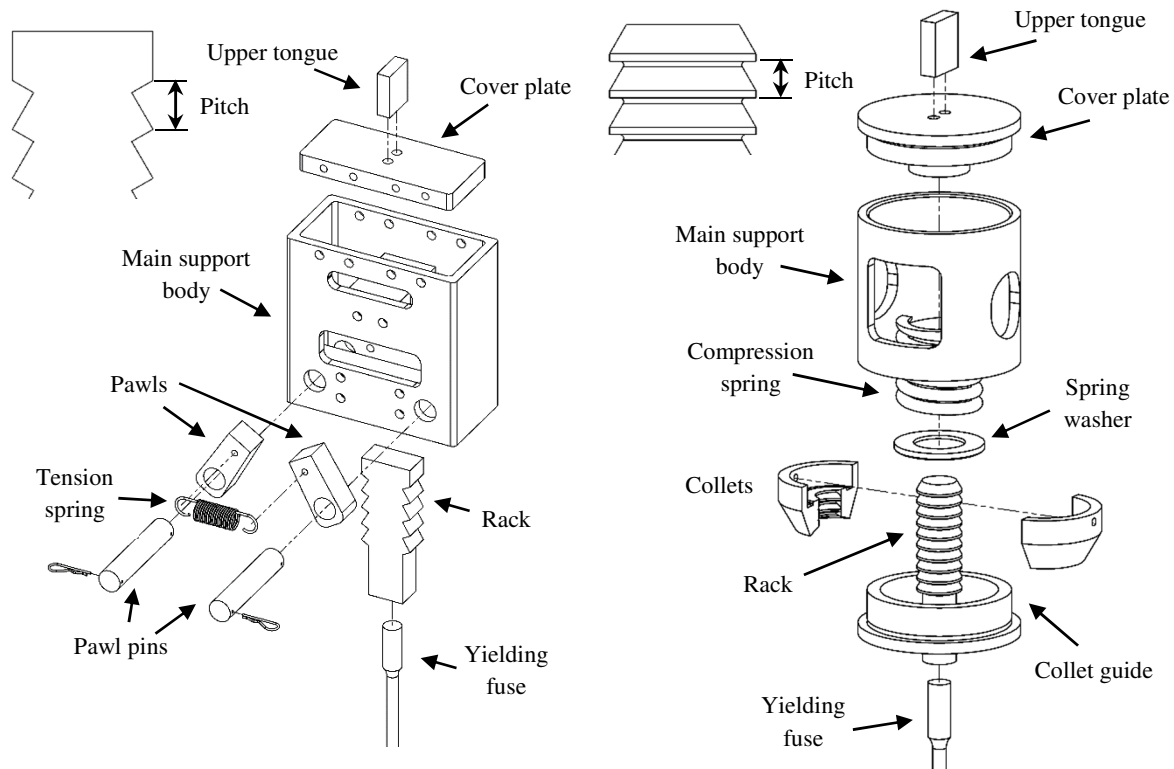

Figure 1a. First, linear ratchet mechanism assembly. Pitch dimension shown in insert.

Figure 1b. Second, axisymmetric prototype. Pitch dimension shown in insert.

The second generation prototype, in Figure 1b, utilises an axisymmetric design. This arrangement enables a reduced tooth pitch and more rapid engagement, with less take-up on initial loading or re-loading. A compression spring acts upon two collets which tighten around a circular rack. The action of these collets replaces the role of the pawls used in the first design. Tensile forces in the fuse are transferred from the rack into compressive forces in the collets and then into the tapered collet guide. Threaded connections are used to connect the collet guide and cover plate to the main support body. The mounting arrangements used with the prototype designs are specific to the hydraulic testing apparatus, and do not limit the possible connection types and applications for the device in service. Racks of four different pitch sizes have been used during the testing of the two prototypes. Pitches of 40 mm and 20 mm were used with the first prototype to establish the concept, while reduced pitches of 10 mm and 3 mm were used with the more advanced, second device. Both prototypes utilise a self-stabilising engagement mechanism. A spring force is used to provide initial engagement before tensile loading forces provide an increased clamping force, ensuring robust and reliable engagement in field structures.

3 EXPERIMENTS AND RESULTS

3.1 Test Apparatus

Experimental proof-of-concept testing on a total of fourteen fuse elements was used to demonstrate the function of the ratcheting mechanism and assess the hysteretic behaviour of the fuse element and the overall device, for both prototypes. High speed camera footage of the ratcheting mechanism was recorded to assess engagement timing with two different pitch sizes for the first, linear prototype. A series of monotonic and cyclic tests were completed with both prototypes in an MTS-810 test machine using the setup shown in Figure 2.
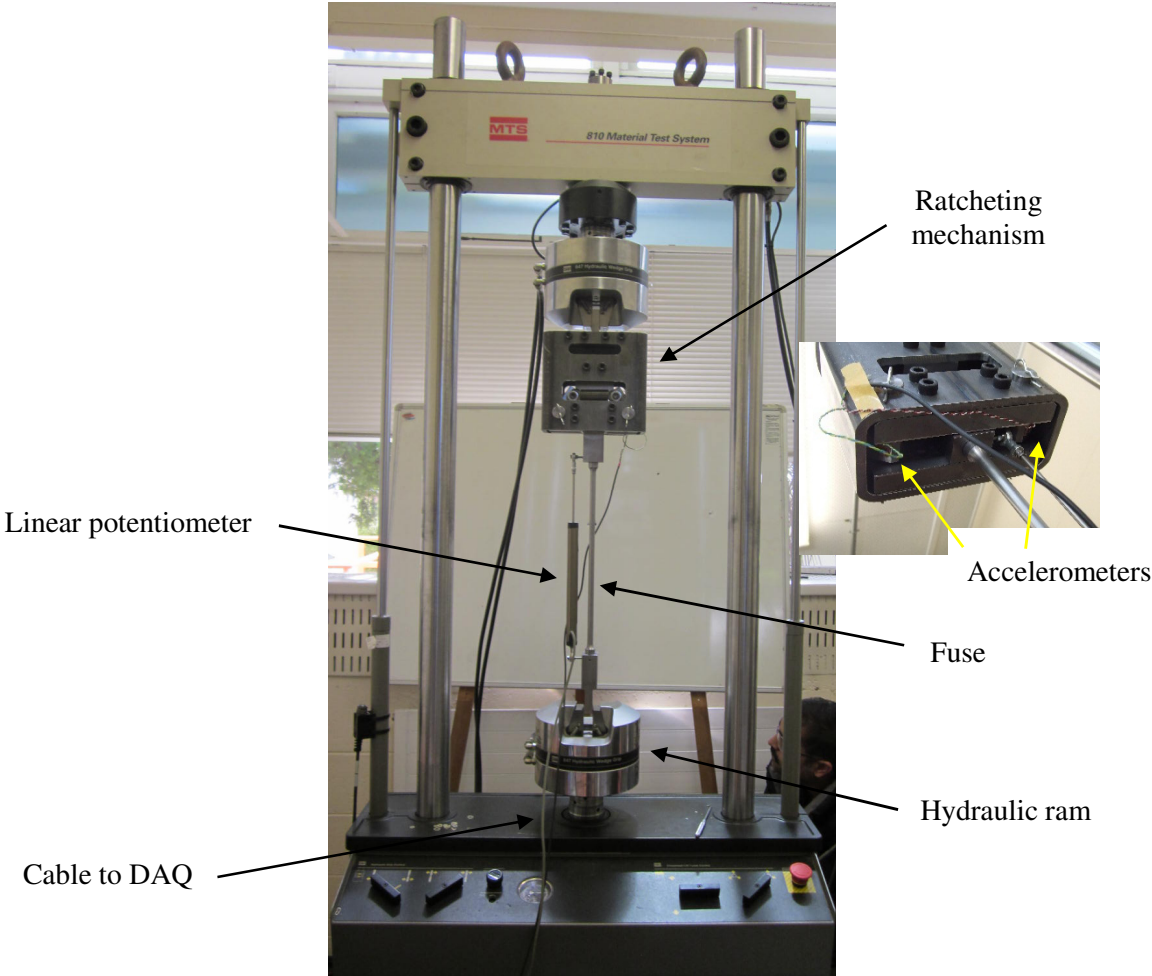

Figure 2. GnG prototype test apparatus. Insert shows accelerometer placement.

3

3.2 Data Acquisition

A data acquisition setup recorded five outputs against time during the experiments. The force and displacement of the hydraulic ram, at the lower end of the device, were recorded from the test machine (the upper crosshead remained stationary). A linear potentiometer position sensor was used to record changes in the length of the fuse element, and was mounted to the device via rod ends bolted to the lower region of the rack and the upper end of the lower tongue, as shown in Figure 2. The remaining two signals were taken from a pair of single-axis accelerometers mounted on the lower ends of the two pawls, shown in the insert in Figure 2. These accelerometers were used to assess pawl engagement timing. All data was sampled at 1000 Hz to ensure all frequencies were captured. High speed camera footage was recorded for several of the tests with the first prototype to measure pawl engagement time using a FASTCAM SA5 model 775K-C3 camera operating at 1000 fps.

3.3 Monotonic Testing

Several tests of monotonic compressive loading were completed to characterise the ratcheting function of the two prototype devices without yielding the fuse elements. During these tests the racks were displaced in compression by at least 50 mm. This enabled the device to ratchet by one tooth when used with the 40 mm pitch rack, and by multiple teeth when used with the smaller pitch racks, up to 22 teeth with the 3 mm pitch rack used with the second, axisymmetric prototype. These tests were completed at different velocities and a summary of the monotonic testing is presented in Table 1, including the maximum compressive forces recorded. Values from different experiments at the same velocity and pitch are separated by a comma.

Table 1. Summary of monotonic compressive testing.

Prototype No.	Pitch (mm)	Velocity (mms^{-1})	Max. Compressive Force (kN)
1	40	50	0.72
		100	1.14
	20	25	0.24, 0.47, 0.47
		50	0.48, 0.76, 0.48
		100	0.32
2	10	25	0.85, 0.89
		50	0.85, 0.96
		75	0.91, 0.76
		100	0.70, 0.77
	3	25	0.73, 0.43
		50	0.73, 0.88
		75	0.82, 0.83
		100	0.84, 0.83

The maximum force experienced by the device during compressive loading, for any of the monotonic tests, was found to be 1.14 kN. This occurred during a test with the first prototype using a 40 mm pitch rack where the ram velocity was 100 mms^{-1}. This result fits with the expectation that slightly larger compressive forces would be experienced by this device during the use of the larger pitch rack. The larger teeth force the pawls to rotate slightly further outward, increasing the tension force in the spring which must be overcome for ratcheting to occur. The second, axisymmetric prototype produced a maximum compressive force of 0.96 kN during the monotonic compressive testing.

3.4 Cyclic Testing

Cyclic tests were also completed to assess the hysteretic behaviour of the fuse element and the overall device. A summary of the cyclic testing parameters is presented in Table 2 and test results in Table 3.

Test amplitudes were selected to clearly present a single ratchetting action during each compressive loading cycle, with the exception of the 3 mm pitch test using an amplitude of 10 mm. This amplitude was chosen to provide a comparison with the behaviour from the 10 mm tooth pitch experiments with the same input displacement amplitude. This comparison is presented later in the paper.

The maximum compressive force experienced by the device during any of the cyclic loading experiments was found to be 1.27 kN. This occurred during a test with the first, linear prototype using a 40 mm pitch rack and operating at 0.25 Hz. The largest compressive force produced by the second, axisymmetric prototype from the cyclic testing was 0.84 kN.In all tests the compressive forces are very low, as intended by design. The experimental values show a reasonable consistency, with an average yield force of 44.0 kN and an average ultimate tensile force of 65.9 kN. The average elongation to fracture was 64.9 mm. This represents ~ 72% of the expected 90 mm elongation at break, indicating that the assumed uniform plastic strain throughout the entire fuse length may not have been obtained during testing. In Table 3, parentheses indicate elongation of fuses that did not fracture during testing.

Table 2. Summary of cyclic testing parameters.

Prototype No.	Pitch (mm)	Amplitude (mm)	Frequency (Hz)	No. Cycles	Ref.
1	40	25	0.25	2	C40-025
			0.50	2	C40-050
	20	15	0.25	3, 3, 3	C20-025
			0.50	3	C20-050
2	10	10	0.50	5, 6	C10-050
			1.00	5, 6	C10-100
			1.50	5, 5	C10-150
	3	10	0.50	4	C03-050
		5	0.50	17	C03-051

Hydraulic test machine limitations (maximum force of 100 kN) dictated the maximum fuse diameter for testing. The ratcheting mechanism is capable of much larger forces if required and exhibited no visible signs of yielding or other damage following testing. While these results use yielding steel fuses for energy dissipation, various dissipation methods, such as friction connections (Clifton 2005) and lead dissipators (Rodgers, et al. 2008), could be implemented with the ratcheting mechanism as required for specific applications and force or yield levels.

Table 3. Summary of cyclic testing results.

Ref.	Yield Force (kN)	Ultimate Tensile Force (kN)	Fuse Elongation to Fracture (mm)	Max. Compressive Force (kN)
C40-025	44.1	66.7	75.2	1.27
C40-050	46.0	67.1	71.4	0.53
C20-025	42.4, 43.5, 46.5	65.1, 65.3, 65.0	65.2, (59.2), (59.3)	0.30, 0.35, 0.28
C20-050	49.9	65.7	71.4	0.49
C10-050	43.3, 43.2	65.9, 66.2	(48.3), 63.1	0.75, 0.84
C10-100	42.9, 43.8	66.0, 66.6	(48.9), 62.7	0.81, 0.73
C10-150	43.3, 45.0	66.5, 66.2	(48.5), 56.9	0.74, 0.80
C03-050	41.5	66.2	57.5	0.46
C03-051	40.7	64.3	60.9	0.32

4 HYSTERESIS BEHAVIOUR

The effect of the ratcheting mechanism produces a unique hysteresis loop for the behaviour of the system. A force displacement plot of the testing with the first prototype, during the cyclic tests with the 20 mm pitch rack, is presented in Figure 3. The input displacement amplitude is 15 mm. The hysteresis loops begin in typical fashion, displaying elastic behaviour, yielding and strain hardening before the first load reversal. During the compressive loading there is an elastic recovery region followed by a period of negligible force. The bottom of the hysteresis loop lies essentially on the horizontal axis, indicating that little force is required for the unloading phase of the cycle.

The value of twice the amplitude of the cyclic loading input exceeds the combined value of the tooth pitch of the rack and the elastic displacement of the fuse. As a result, the displacement at which the GnG device engages during the next loading cycle is reduced by an amount equal to the tooth pitch. This is shown in Figure 3 where it can be seen that during the unloading phase of the initial cycle, the displacement is approximately 13 mm after elastic recovery. During the following cycle the onset of elastic strain behaviour of the system occurs at a displacement of approximately - 7 mm, with respect to the initial position. It is observed that similar behaviour occurs for the other two loading and unloading cycles, with a slight change in position due to an increase in elastic displacement as a result of the increased force from strain hardening. The hydraulic ram reaches a minimum position of -15 mm, and Figure 3 indicates that up to 8 mm of free-travel exists before engagement of the rack and pawls. Similar behaviour was exhibited in tests with the larger pitch rack, with around 7 mm of free-travel on reloading.

In Figure 3, it is shown that from a displacement of -15 mm to -7.5 mm, reloading occurs without much resistive force. This free-travel $x_{free-travel}$ is directly proportional to tooth pitch p and can be approximated by Equation 1 (where it is assumed that $p < 2A < 2p$):

$$x_{free-travel} = 2A - p - \delta_{elastic} \tag{1}$$

where A is the amplitude of the displacement input cycle and $\delta_{elastic}$ is the elastic displacement recovered by the device during unloading. These terms are expressed in Figure 3. The engagement displacement values are consistent for tests with the same rack due to approximately equal starting positions, with the rack resting on the closed pawls. Multiple ratcheting actions can occur when $2A > 2p$.
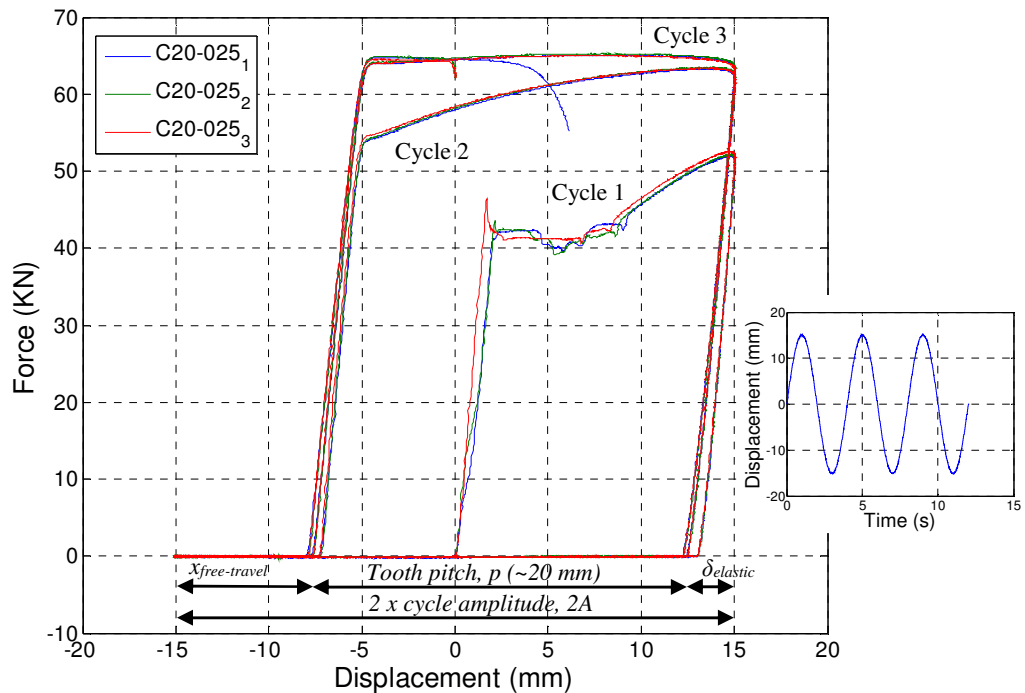

Figure 3. Force displacement hysteresis loops for cyclic testing of 20 mm pitch rack. The input displacement profile is inset.

6

This result differs from the expected behaviour of a regular yielding steel hysteresis loop due to the ratcheting mechanism essentially shifting the zero displacement datum. The amount of free-travel prior to re-engagement of the yielding mechanism on subsequent cycles is reduced due to the absence of compressive loads, and the displacement does not need to exceed that experienced on prior cycles before energy dissipation can occur, as is a limitation with simple tension bracing. The onset of tensile yielding of the GnG device occurs when the force in the fuse exceeds the force at the start of the unloading phase in the previous cycle. While the test was cyclic, the steel yields only in tension and the behaviour approximates a monotonic tensile test.

Figure 4 compares the hysteretic behaviour of the second prototype using 10 mm and 3 mm pitch racks for cyclic loading with a reduced input displacement amplitude of 10 mm. It is seen in Figure 4 that the re-engagement of the device on subsequent loading cycles occurs at a displacement of approximately - 3 mm, with respect to the initial position, when using a pitch of 10 mm. This engagement displacement is changed to approximately -7 mm when using the finer 3 mm pitch rack, representing a 7mm to 3mm reduction in the uptake that occurs prior to engaging the energy dissipation mechanism. It is clear that the enclosed area for the finer pitched rack has increased by ~50%, demonstrating a significant increase in energy dissipation for the same displacement loading input.
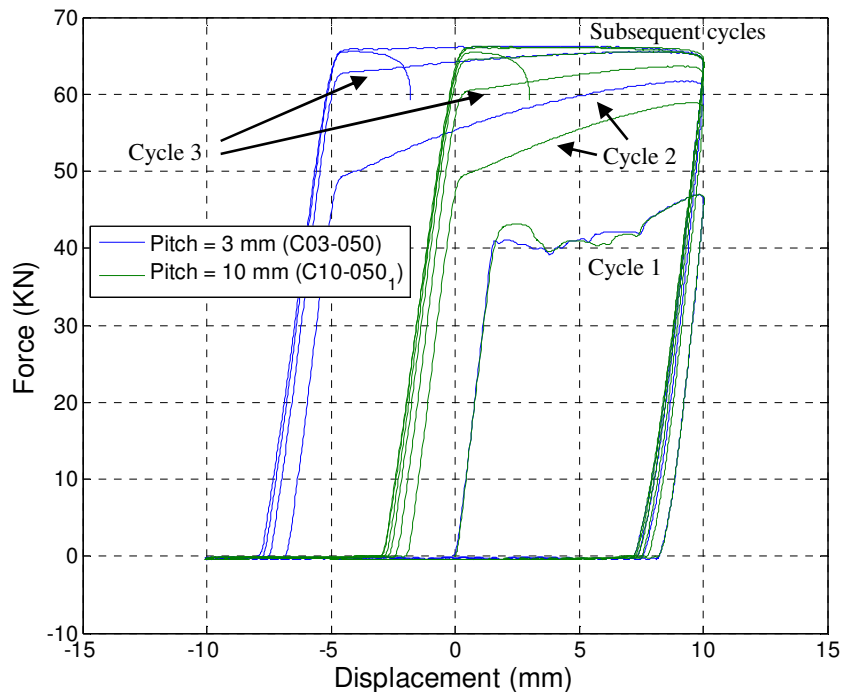

Figure 4. Comparison of take-up reduction with use of finer pitch rack in second prototype.

This ratcheting GnG system has applications in seismic energy dissipation, and could replace a traditional yielding steel device and reduce take-up between loading cycles, resulting in more rapid engagement of the energy dissipation system. This faster response will reduce shock/impact loads and maximise the amount of energy absorbed by the device, thus minimising the response of the structure and the effects of earthquake loading. It should be noted that a smaller tooth pitch will reduce the amount of free-travel and the magnitude of any impact loading, but will also increase the cumulative plastic displacement demand in the fuse element. As with traditional steel fuses, the total displacement capacity of the GnG device is limited by the available plastic displacement of the fuse prior to fracture. Variation in size and design of the fuse can provide greater displacement capacity to suit specific applications.

5 CONCLUSIONS

A ratcheting, tension-only fuse device has been developed to offer resistance to loading in tension, while offering negligible resistance to compressive motion. This lack of compressive forces allows re-seating of a rocking connection and minimises residual structural displacements. Upon reloading, fuse

engagement will be more rapid than a simple steel fuse due to the ratcheting mechanism, as the absence of residual compressive loads reduces the amount of elastic take-up before yielding occurs. This effect leads to greater energy dissipation. Moreover, in post-tensioned rocking systems residual compressive forces partially offset the clamping effect of the post-tensioning. Therefore, the overall resistance to the onset of rocking may be reduced for subsequent cycles using a traditional yielding steel component such as a BRB. The GnG device eliminates this effect for consistent, repeatable rocking behaviour.

A hysteresis model has been developed to capture the behaviour of the ratcheting fuse mechanism, and simulations are in progress to demonstrate the effect of the devices on structural response to earthquake loading, and to quantify the cumulative yield displacement demand on the fuse element.

6 ACKNOWLEDGEMENTS

REFERENCES:

Black, C.J. Makris, N. & Aiken, I. 2004. Component testing, seismic evaluation and characterization of buckling-restrained braces, *Journal of Structural Engineering*, 130(6): 880-894.

Canterbury Earthquakes Royal Commission. 2012. *Low-damage Building Technologies*. Christchurch, NZ.

Clifton, G.C. 2005. *Semi-rigid joints for moment-resisting steel framed seismic-resisting systems*, PhD Thesis, The University of Auckland, Auckland, New Zealand.

Eatherton, M.R. Fahnestock, L.A. & Miller, D.J. 2014. Self-centering buckling restrained brace development and application for seismic response mitigation, *10th U.S. National Conference on Earthquake Engineering: Frontiers of Earthquake Engineering, NCEE 2014, Anchorage, Alaska, 21-25 July, 2014*.

Gunning, M. & Weston, D. 2013. *Assessment of Design Methodologies for Rocking Systems*, ENCI493 Report, Supervised by MacRae, G.A., Dept of Civil and Natural Resources Eng, Univ of Canterbury, Christchurch, NZ.

Hao, H. 2015. Development of a New Nonbuckling Segmented Brace. *International Journal of Structural Stability and Dynamics,* 15(8): Article in Press.

Kang, J.D. & Tagawa, H. 2013. Seismic response of steel structures with seesaw systems using viscoelastic dampers. *Earthquake Engineering and Structural Dynamics*, 42(5): 779-794.

Kanitkar, R. Aiken, I.D. Nishimoto K. & Kasai, K. 2006. Viscoelastic dampers for the seismic retrofit of buildings: An overview of advancements in viscoelastic materials and analytical capabilities, Paper No. 1299, *Proc. 8th U.S. National Conference on Earthquake Engineering, EERI, Oakland, Calif., 18-22 April, 2006*.

Lee, D. & Taylor, D.P. 2001. Viscous damper development and future trends, *Structural Design of Tall Buildings,* 10(5): 311-320.

Lei, J.S. Luo, W.X. Jiang, J.L. Zhang, W. 2014. Seismic performance analysis of steel frame with wedge devices based on energy dissipation, *4th International Conference on Civil Engineering, Architecture and Building Materials, CEABM 2014, Haikou, China, 24-25 May, 2014*.

New Zealand Treasury. 2014. *2014 Budget: Budget Policy Statement.* Wellington, New Zealand.

Phocas, M.C. & Pocanschi, A. 2003. Steel frames with bracing mechanism and hysteretic dampers. *Earthquake Engineering and Structural Dynamics,* 32(5): 811-825.

Rodgers, G.W. Solberg, K.M. Chase, J.G. Mander, J.B. Bradley, B.A. Dhakal, R.P. & Li, L. 2008. Performance of a damage-protected beam-column subassembly utilizing external HF2V energy dissipation devices, *Earthquake Engineering and Structural Dynamics*, 37(13): 1549-1564.

Symans, M.D. Charney, F.A. Whittaker, A.S. Constantinou, M.C. Kirhcer, C.A. Johnson, M.W. & McNamara, R.J. 2008. Energy dissipation systems for seismic applications: Current practice and recent developments, *Journal of Structural Engineering*, 134(1): 3-21.